The Microelectrode Insulator Influences Water Droplet Collisions

Kathryn J. Vannoy^a, Christophe Renault^a, and Jeffrey E. Dick^{a,b}*

^aDepartment of Chemistry, Purdue University, West Lafayette, IN 47907, USA ^bElmore Family School of Electrical and Computer Engineering, West Lafayette, IN 47907, USA

*jdick@purdue.edu

Abstract: Studying chemical reactions in very small (attoliter to picoliter) volumes is important in understanding how chemistry proceeds at all relevant scales. Stochastic electrochemistry is a powerful tool to study the dynamics of single nanodroplets, one at a time. Perhaps the most conceptually simple experiment is that of the current blockade, where the collision of an insulating particle is observed electrochemically as a stepwise decrease in current. Here, we demonstrate that nanodroplet collisions on microelectrodes are not as simple as water droplets adsorbing to the electrode to block current, and that the environment immediately around the microelectrode (glass insulator) plays a pivotal role in the electrochemical collision response. We use correlated opto-electrochemical measurements to understand a variety of electrochemical responses when water nanodroplets collide with a microelectrode during the heterogeneous oxidation of decamethylferrocene in oil. The amperometric current reports not only on current blockades but also nanodroplet coalescence events and preferential wetting to the glass around the microelectrode. Treating the glass with dichlorodimethylsilane creates a hydrophobic environment around the working electrode and the simple current blockade response expected from the absorption of insolating nanoparticles is observed. These results highlight the importance of the environment around the working electrode for nanodroplet collision studies.

Introduction:

For over a decade, electrochemistry has been used to study the reactivity and dynamics of single nanoparticles by their stochastic interaction with an electrified microinterface. Such experiments have allowed for the study of industrially important inner-sphere reactions at single nanoparticles¹⁻⁴, development of new methods for nanoparticle synthesis⁵⁻⁶, complex electrochemical processes on 2D materials⁷, and the realization of ultrasensitive biosensors capable of single molecule detection^{8,9}, and the elucidation of accelerated enzyme kinetics.¹⁰ The impacting particles tend to be on the order of nanometers-micrometers, and can be comprised of a wide variety of materials; including metal nanoparticles, viruses, and liquid droplets. This report aligns most closely with "blocking" experiments, or the impact of an insulating material.

In 2004, Lemay and co-workers described an electrochemical means by which one could observe the real-time adsorption of single microspheres on microelectrodes. ¹¹ They observed a sudden decrease (*i.e.*, step down) in current of ferrocenemethanol oxidation at a microelectrode

surface when an insulating microsphere irreversibly adsorbed on the surface. These experiments opened the floodgates to the field of stochastic electrochemistry. In 2020, Lemay and Thorgaard independently described such events by tracking charged polystyrene beads¹² and bacteria¹³, respectively, under electro-osmotic conditions. The authors used correlated microscopy to understand the additional transient current blocking events (*i.e.*, spikes, blips) observed in the current-time trace.

Stochastic electrochemistry is also a convenient means by which one can study single sub-femtoliter nanodroplets. Many groups have used the technique to study the reactivity of the nanodroplet contents. However, there are fewer experiments that look at the dynamics of the reactor during the collision event. Similar to the detection of hard nanoparticles, by driving a heterogenous reaction at the microelectrode surface, soft nanoparticles can block reactant flux as they approach and irreversibly wet the surface, resulting in a decreased steady-state current response. Blocking-type experiments have been used to count, one-at-a-time, the adsorption of single molecules, viruses, bacteria, and vesicles suspended in aqueous conditions. Several groups have demonstrated the current decrease (step down) response for various oil nanodroplets-in-water systems and in 2017 Kim and Park demonstrated the "step down" collision responses for water droplets-in-oil.

Previously, our group used correlated optical and fluorescence microscopy to quantify properties of 2D nanomaterials colliding on microelectrodes.^{28,29} We were able to see various transients as the nanoparticle interacted with the diffusion layer during a collision event.

Here, we demonstrate that the blocking experiment with water micro- and nanodroplets does not result only in the blocking steps previously observed with insulating particles. When we drive the oxidation of decamethylferrocene in 1,2-dichloroethane (DCE) and suspend aqueous nanodroplets, the current transients present a variety of unexpected responses. Under our conditions, which are similar to the conditions previously reported, we show four common electrochemical responses: the blocking step, transient blocking, transient blocking followed by an increase in anodic current, and transient increases. This is the first report that demonstrates that an insulating nanoparticle collision can increase the current. With correlated optical and fluorescence microscopy, we discover the origin of these additional transients, and highlight the importance of correlated experiments and the environment around the working electrode in stochastic electrochemistry.

Materials and Methods:

Bis(pentamethylcyclopentadienyl) iron (II) (decamethylferrocene, 97%), tetrabutylammonium perchlorate (TBAP, \geq 99%), and fluorescein sodium salt were purchased from Sigma Aldrich (St. Louis, MO). 1,2-dichloroethane (DCE, HPLC grade >99%) was purchased form Thermo Fisher (Ward Hill, MA). Acetone, Potassium Chloride (KCl, >99%), and agarose were obtained from Fisher (Fair Lawn, NJ). Silanization solution I (~5% dimethyldichlorosilane in heptane) was purchased from Supelco (Bellefonte, PA). Water (18.20 M Ω •cm) was obtained from a Barnstead GenPure Milli-Q water purification system, which was purchased from Thermo Scientific (Waltham, MA).

A CH Instruments (Austin, TX) potentiostat (either 6284 or 920 series) was used to make all electrochemical measurements. The working electrode was a gold microelectrode (d = 12.5 μ m), a gold SECM tip (d = 12.5 μ m), or a platinum microelectrode (d = 10 μ m), purchased from CH Instruments. The reference electrode was a 1 M KCl Ag/AgCl electrode from CH

Instruments. The counter electrode (for benchtop amperometry) was a platinum coil (d = 1 mm) from GoodFellow (Pittsburg, PA).

Optical microscopy was performed using a Leica DMi8 inverted microscope (Leica Microsystems, Germany), and a Hamamatsu ORCA-Flash 4.0 (C13440) Digital sCMOS camera (Hamamatsu, Japan). The objective used was Leica HC PL Fluotar 40X/0.6 with an additional internal 1.6X swqlens. The optical images were obtained under brightfield illumination or fluorescence by a Leica GFP filter cube (11525314). For correlated electrochemical analysis, a stepper and piezo positioner/controller (CH Instruments mounted on the microscope stage was used to position the microelectrode at about 350 μ m above the coverslip. The optoelectrochemical cell consisted in a N°0 coverslip (bottom of the cell) glued onto a glass cylinder containing the solution. The positioner/controller is controlled through the 920D bipotentiostat (CH Instruments). HCImage live software (Hamamatsu) and ImageJ (open source) were used for micrograph analysis.

Typical emulsion preparation

 $40~\mu L$ of water (with or without 1 mM fluorescein) was pipetted into a glass vial, and 10 mL of 1 mM decamethylferrocene, 5 mM tetrabutylammonium perchlorate (TBAP) in 1,2-dichloroethane (DCE) was added. The solution was sonicated by a Q500 horn ultrasonicator from QSonica (Newton,CT). A pulsed cycle of 5 s on, 5 s off (amplitude 40%) for one minute was used to create the emulsion.

Amperometry

For benchtop amperometric experiments (Figure 1): a three-electrode system was used with a CHI 6284 potentiostat. The working electrode was a gold microelectrode ($d = 12.5 \mu m$), the counter electrode was a platinum coil, and the reference electrode was a Ag/AgCl (1 M KCl) connected the electrochemical cell by a salt bridge. The salt bridge was a glass capillary filled with 3% w/w agarose/1 M KCl. 5 mM TBAP was added in the continuous phase to minimize resistance in the low dielectric media. Before each experiment, cyclic voltammetry was performed in the continuous phase to determine the potential where the current is limited by mass-transfer and check the electrode.

For all amperometric experiments correlated with microscopy: a two-electrode system was used by connecting both the counter and reference lead to the Ag/AgCl reference electrode (connected to the cell by a salt bridge). A SECM tip gold microelectrode (*d* = 12.5 μm) was used as the working electrode to avoid the surrounding glass blocking a lot of the droplet flux to the surface when the electrode was placed close to the bottom of the cell. A CHI 920 potentiostat with a micropositioning system was used. Before each experiment, cyclic voltammetry was performed in the continuous phase (1 mM decamethylferrocene, 5 mM TBAP/DCE) to determine the potential where the current is limited by mass-transfer and check the electrode. Figure S1 shows the cyclic voltammograms obtained before the amperometry experiments. After the cyclic voltammetry, the continuous phase was removed, and the emulsion was pipetted into the electrochemical cell. The experiment was started immediately after the addition of the emulsion. A potential of 0.3 V vs salt bridge|Ag/AgCl (1 M KCl) was applied, sampling every 50 ms. A quiet time of 2 s was used to avoid recording the initial capacitive decay. The amperometry was triggered by a TTL signal from the camera to ensure synchronization.

Between each amperogram, the microelectrode was gently polished on a polishing microcloth with $0.05~\mu m$ alumina powder slurry, and then on a clean, wet polishing pad to

remove the alumina. The microelectrode was rinsed with water and acetone and was dried prior to the experiment.

The silanization was performed by dipping the microelectrode into the silanization solution for approximately 30 s. The microelectrode was allowed to air dry and then was rinsed thoroughly with ethanol, water, and acetone, and was dried prior to the experiment.

Microscopy

Fluorescence microscopy (GFP filter cube, excitation 470/40 nm, emission 525/50 nm) was used to track fluorescein (excitation 460 nm 30) that was loaded into the water droplets. Magnification of 40X with an additional 1.6X was used for all correlated experiments. The microelectrode was placed approximately 350 μ m in plane above the cover slip by a micropositioning system in the 920 CHI potentiostat. The exposure time was 50 ms, such that each captured image corresponds to a point on the amperogram.

Results and Discussion:

In our experiments, we oxidize 1 mM decamethylferrocene (a hydrophobic one-electron mediator) using mass transfer-limited potentials at a gold microelectrode ($d=12.5~\mu m$) in 1,2-dichloroethane (DCE) containing 5 mM tetrabutylammonium perchlorate (TBAP). Supporting Information Figure S1 shows representative cyclic voltammograms obtained before amperometry. An emulsion ($\sim 0.4\%~v/v$ water/DCE) was prepared by the ultrasonication of water with 1 mM decamethylferrocene and 5 mM TBAP in DCE, creating a dispersion of water nanoand microdroplets suspended in the DCE phase. Amperograms were recorded for several minutes while water nano- and microdroplets collided with the submerged microelectrode (Figure S2). A schematic showing the electrochemical oxidation of decamethylferrocene in DCE at the microelectrode surface in the presence of water nanodroplets is shown in Figure 1A. The diffusion layer is represented in green, and represents the presence of the oxidized species, decamethylferrocenium. Figure 1B shows the first 60 s of an amperogram, where we observe current blocking steps (Figure 1C), but also three other transient shapes, including transient blocking spikes (Figure 1D), transient blocking and transient extra current (Figure 1E), and transient extra current spikes (Figure 1F).

In line with previous reports, stepwise current decreases are observed. This response is what one would expect when a nanodroplet irreversibly adsorbs to the electrode surface while a heterogeneous reaction is being driven. A water droplet approaches the microelectrode and wets the surface, such that the adsorbed water blocks a portion of the microelectrode surface, decreasing the observed current. For hard nanoparticles (e.g., polystyrene beads) the step magnitude is often used to calculate the size of the impacting particle by relating the change in the limiting current to the change in the effective radius of the electrode ($i_{limiting} \alpha r_{electrode}$). However, this calculation is plagued by the non-uniform flux profile at the microelectrode surface (i.e., the edge effect). This analysis is further complicated for droplets, or nanoparticles with a soft interface, where one would have to assume a relationship between wetting and droplet volume. Thus, in these experiments, a correlated technique (e.g., microscopy) is needed to rigorously know the size of the insulating droplet.

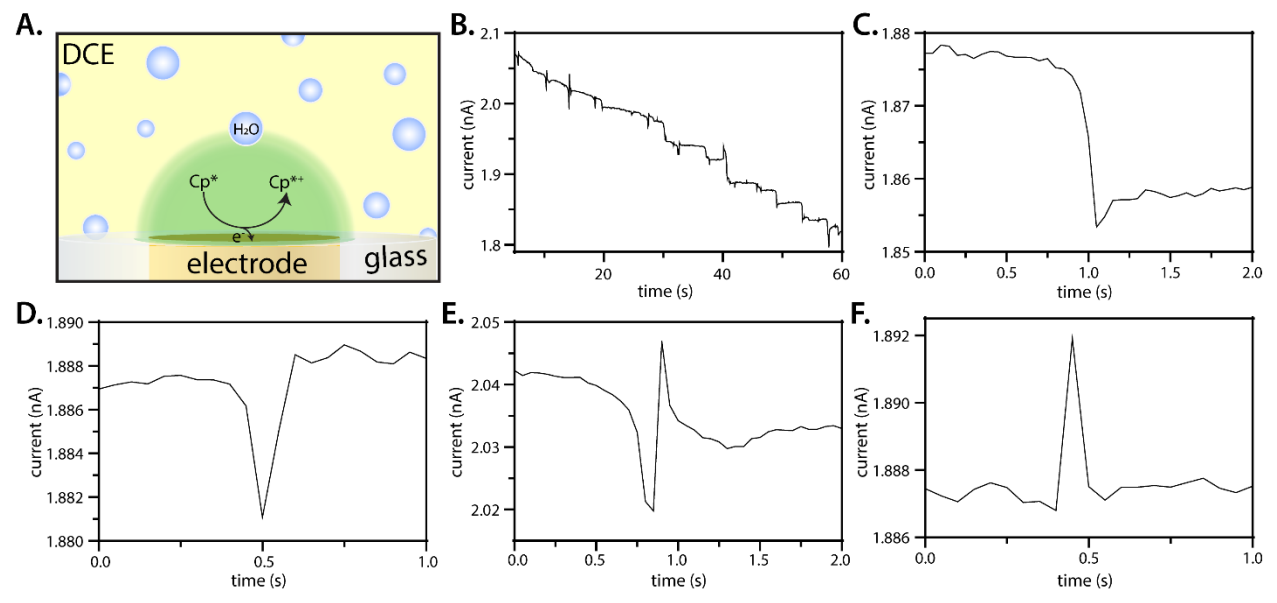


Figure 1. Amperometric experiment. **(A)** Schematic showing the gold microelectrode biased to oxidize decamethylferrocene in DCE with suspended water nano- and microdroplets. A three-electrode system comprised of a gold microelectrode (*d* = 12.5 μm),salt bridge|Ag/AgCl reference, and platinum wire counter. Water was emulsified into 1 mM decamethylferrocene in 5 mM TBAP DCE. **(B)** Representative amperogram where the gold microelectrode was biased at 0.3 V *vs* Ag/AgCl. **(C-F)** Event shapes observed in panel B amperogram. The time was background-subtracted to show the duration of the event. **(C)** Sustained blocking event (panel B from 48.0 s to 50.0 s). **(D)** Transient blocking event (panel B from 41.5 s to 42.5 s). **(E)** Transient blocking and transient increase (panel B from 9.5 s to 11.5 s). **(F)** Transient increase (panel B from 43.5 s to 44.5 s).

Along with the sustained current-blocking events, transient events that only affect the current over milliseconds-seconds are frequently observed in the amperogram. In fact, the simple step-down response makes up only about 50% of the observed transients (counted over three-minutes). Figure 1B shows a transient blocking event, or a spike-type response returning to baseline, that can be explained by nanodroplets entering and exiting the diffusion layer without contacting the microelectrode surface. Lemay and Thorgaard demonstrated similar events occurring during electro-osmotic flow^{12,13}, which deflected particles before collision with the microelectrode surface. In our experiments, the concentration of electrolyte in the oil phase is 5 mM and the redox mediator was 1 mM decamethylferrocene. In previous reports electro-osmotic effects appeared in amperometric signals when the supporting electrolyte concentration was lower than the redox mediator concentration. Nanoparticles follow a specific trajectory under electro-osmotic flow, and we did not observe such a trajectory in our correlated microscopy experiments (vide infra).

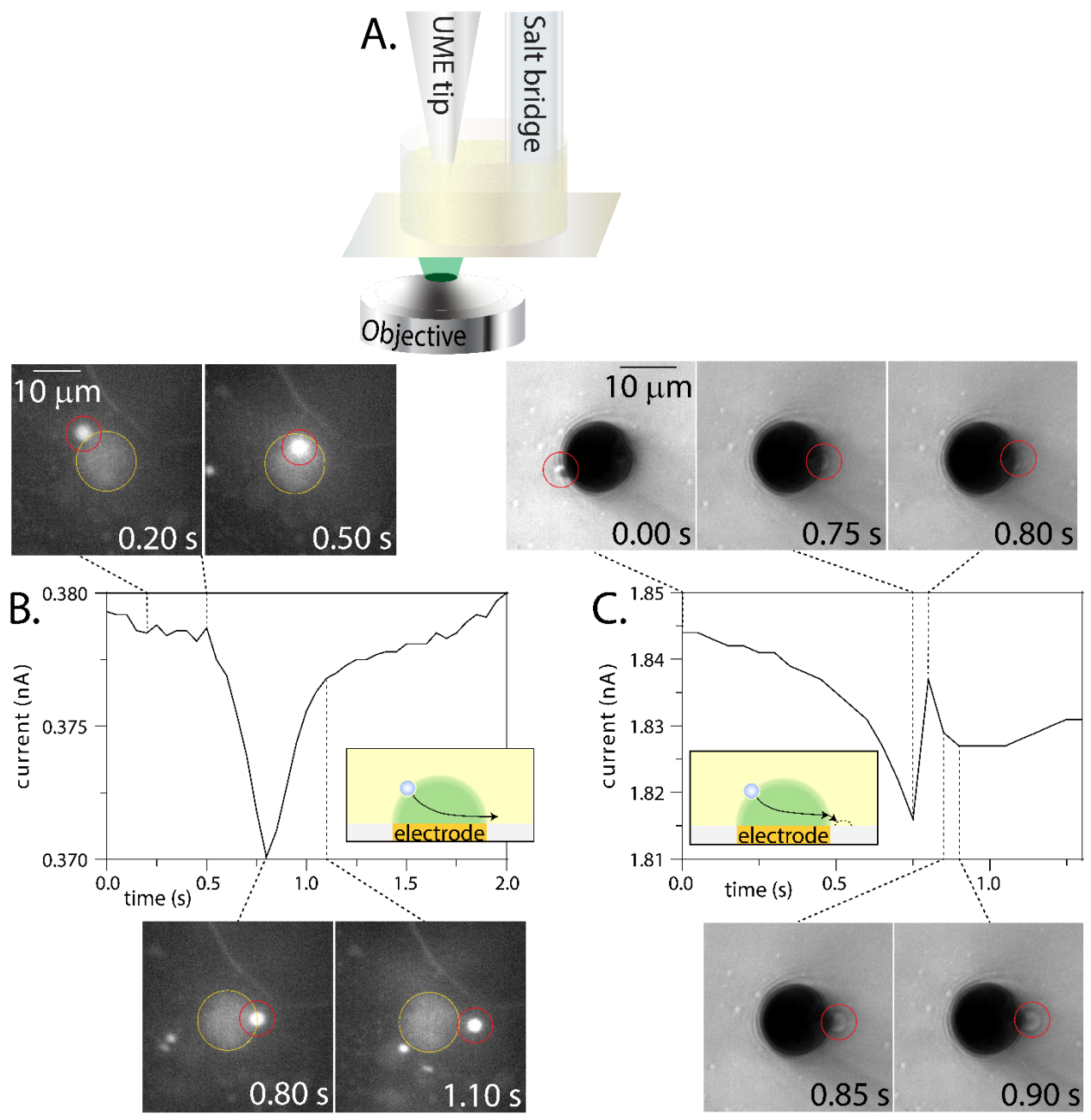


Figure 2. A water droplet passes over the microelectrode surface. **(A)** Schematic showing the objective in plane with the microelectrode surface and the two-electrode system comprised of a gold microelectrode ($d = 12.5 \, \mu m$) and salt bridge|Ag/AgCl counter/reference.1 mM fluorescein in water was emulsified into 1 mM decamethylferrocene in 5 mM TBAP DCE. **(A-B)** In all the micrographs in this figure, the gold microelectrode is outlined in yellow and the incoming water droplet is circled in red. 0.3 V vs reference was applied to the microelectrode and the sampling rate was 0.05 s. Micrographs were collected with a 40X/0.6 objective and 1.6X magnification. For each amperogram, anodic current is represented as positive and the time was background subtracted to show the duration of the individual event. The inset schematics suggest a profile view of the observed transient. The yellow represents decamethylferrocene in DCE, the green represents decamethylferrocenium in DCE, and the blue represents the water droplet. **(A)** Fluorescence microscopy was recorded by use of a GFP filter cube. The micrograph panels correspond to 0.20 s, 0.50 s, 0.80 s, and 1.10 s. These time points are also shown by colored dashed lines on the amperogram. **(B)** Microscopy was collected in brightfield. The illumination caused a shadow visible around the microelectrode. The micrograph panels correspond to 0.00 s, 0.75 s, 0.80 s, 0.85, and 0.90 s. These time points are also shown by colored dashed lines on the amperogram.

is not immediately obvious how an empty water droplet could provide an increase in the anodic current under mild potentials. Importantly, the same transients are observed under high salt conditions (250 mM TBAP).

These transients are difficult to understand by the electrochemical information alone. To elucidate these responses, we tracked the nanodroplets as they approach the microelectrode surface with optical and fluorescence microscopy, either by using brightfield imaging or 1 mM fluorescein added into the nanodroplets. A schematic of the experimental setup is shown in Figure 2A. With the correlated data, we describe below what gives rise to these less intuitive current-time transients.

Figure 2B-C confirms that the current can respond to a passing particle that never contacts the microelectrode. When a droplet passes closely over the microelectrode but does not wet, there is transient blocking of the anodic current by the droplet inside the diffusion layer. Figure 2B provides a series of fluorescence micrographs of this event type correlated with amperometry (current-time). The spike of decreased anodic current can be explained by the incoming droplet transiently blocking the flux of decamethylferrocene to the microelectrode surface as it passes by.³³ The most blocking (minimum current) occurs as the droplet passes over the edge of the microelectrode (0.8 s, Figure 2B), where there is a higher relative flux. The absence of a spike-type response as the droplet first crosses over the microelectrode (0.02 s, Figure 2B) and the slow current decrease suggests that the droplet is also approaching the microelectrode in the z-dimension between the timepoints. The descent is further evidenced by the droplet appearing more in focus at the last time-point compared to the first, indicating that it approaches the focal plane (i.e., the microelectrode surface) over this time. The proposed profile view of this response is illustrated by the inset schematic. Previously, Hui and co-workers³⁴ claimed that water nanodroplets may fission after colliding with a microelectrode. In this work, we saw no evidence of droplet fission.

Figure 2C also shows a nanodroplet passing over the microelectrode. However, instead of staying suspended, the nanodroplet rapidly wets the glass that insulates the microelectrode disk. These micrographs were collected with brightfield microscopy. Again, when the droplet passes over the microelectrode surface, there is a decrease in current (0.00 s to 0.75 s, Figure 2C). However, here the droplet gets close enough to the hydrophilic glass, and it jumps to wet, rapidly removing it from the diffusion layer. A spike of anodic current beyond the baseline is observed at 0.80 s. We hypothesize that the fast wetting can provide convection that increases the flux of decamethylferrocene towards the microelectrode surface, transiently increasing the anodic current. We also observe that the droplet can rearrange on the surface after wetting (0.80 s to 0.90 s), and often arranges to further wet the glass surface. The duration of the electrochemical blocking responses shown in Figure 2 are dependent on the time that the droplet spends in the diffusion layer. The droplet velocity was calculated by tracking the individual droplets as they travel in the plane with the microelectrode surface. Velocities of 13.9 μ m/s and 15.6 μ m/s were calculated for the droplets shown in Figure 2A (diameter 2.6 μ m) and Figure 2B (diameter 3.4 μ m), respectively.

Figure 3 shows events that occur after about one minute of collisions, where the microelectrode was nearly covered by a pool of water (see Supporting Information Figure S3 for the covering event). The microelectrode perimeter is outlined with a yellow circle for clarity. Without microscopy, one might assume that the collisions must be occurring with the small amount of electrode that remains uncovered by water; however, optical correlation indicates that

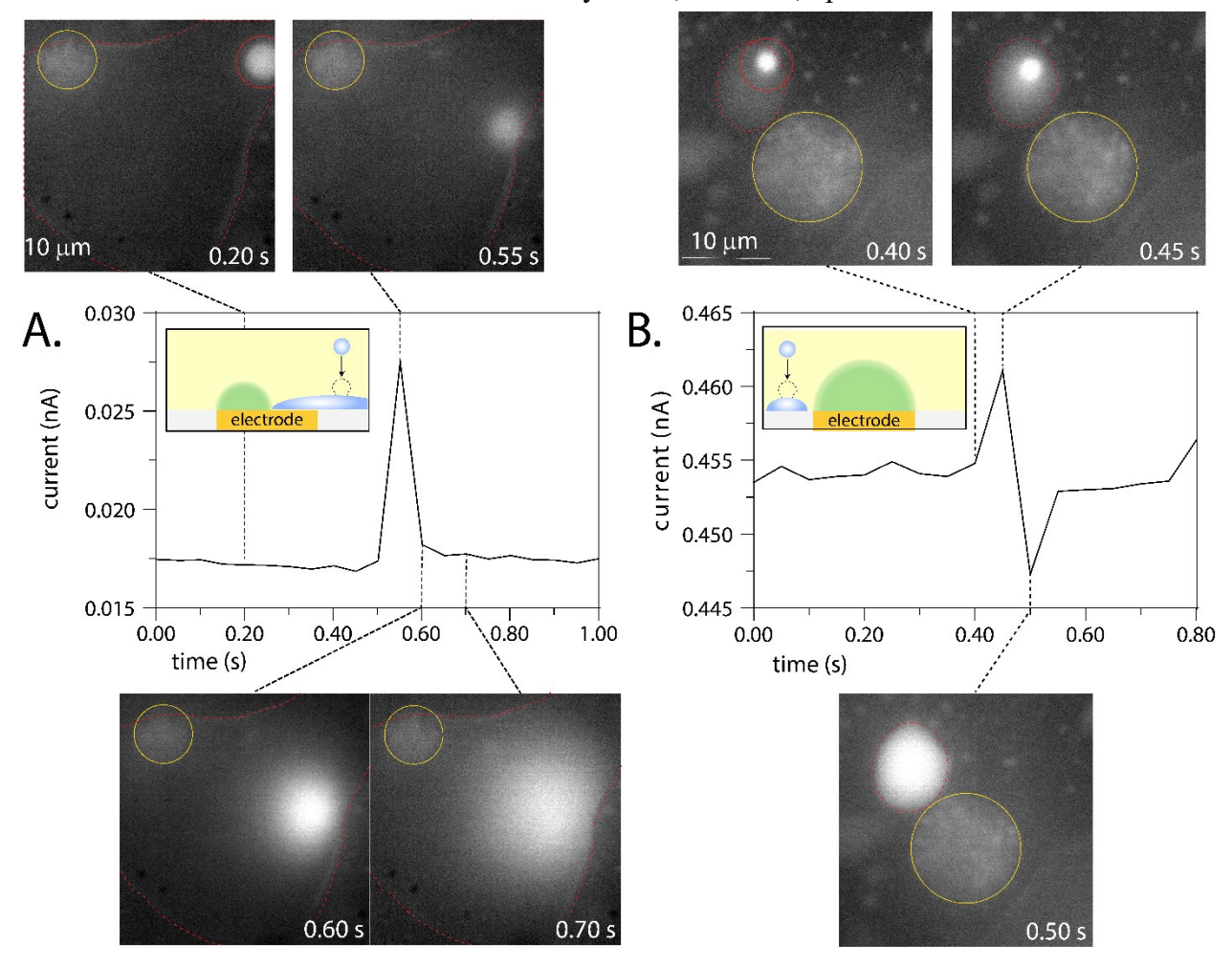


Figure 3. A water droplet containing 1 mM fluorescein coalesces with adsorbed water. A two-electrode system was used with a gold microelectrode and salt bridge|Ag/AgCl counter/reference in a 1 mM decmethylferrocene in 5 mM TBAP DCE. 0.3 V vs reference was applied and the sampling rate was 0.05 s. (**A-B**) In all the micrographs in this figure, the gold microelectrode ($d = 12.5 \mu \text{m}$) is outlined in yellow, the adsorbed water is outlined in whited dotted lines, and the incoming water droplet is circled in red. Micrographs were collected with a 40 X/0.6 objective and 1.6 X magnification. The inset schematics suggest a profile view of the observed transient. The yellow represents decamethylferrocene in DCE, the green represents decamethylferrocenium in DCE, and the blue represents the water droplet. Anodic current is represented as positive in the amperograms. (**A**) The left panel corresponds to 0.20 s, the second panel corresponds to 0.55 s, the third panel corresponds to 0.60 s, and the last panel corresponds to 0.40 s, the second panel corresponds to 0.45 s, and the last panel corresponds to 0.40 s, the second panel corresponds to 0.45 s, and the last panel corresponds to 0.50 s. These time points are also indicated by dashed lines on the amperogram.

transients that could easily be mistaken for droplet|electrode collisions based on the amperometric signal are actually droplet-droplet fusion events. As soon as a droplet has landed on or near the electrode, there is the potential for coalescence/fusion for any subsequent droplet

that approaches. Due to the height of the adsorbed droplet, incoming droplets may coalesce instead of wetting the surface of the microelectrode or glass.

Figure 3 demonstrates two additional examples that provide a transient increase in the current response. Figure 3A shows a droplet fusion event, where an incoming droplet coalesces with a droplet already adsorbed to the microelectrode surface. This results in a blip of anodic current at the moment of coalescence (0.55 s, Figure 3A). The moment of coalesce is taken as the time point before the fluoresce spreads across the adsorbed droplet. Here, the volume of the incoming droplet is much less than the adsorbed water and the droplet coalesces far from the microelectrode surface/diffusion layer. We also note that the droplet is out of focus even as is coalesces, indicating it is well above the plane of the electrode. The increase in fluorescence intensity after coalescence could be due to the fluorophores diffusing into better focus or an electrochemical effect from contact with the biased electrode. Figure 3B shows a droplet fusion event, where the incoming droplet coalesces with a droplet adsorbed to the glass just outside the perimeter of the microelectrode surface. Again, we observe a blip in anodic current at the moment of coalescence (0.45 s, Figure 3B), but here it is immediately followed by a spike-type reduction in anodic current. In both cases, we suspect a rearrangement of the adsorbed water as it fuses with the incoming droplet. We hypothesize that the increased current arises from either a temporary decrease in the contact area of the adsorbed droplet, as it reaches to wet the incoming droplet, or fusion-based convection along the microelectrode|DCE|adsorbed droplet boundary. Interestingly, Figure 3A demonstrates that a droplet can be electrochemically sensed tens of micron from the microelectrode surface. Previously, Samec and co-workers showed that droplet collisions with a larger droplet could be observed with open circuit measurements relying on the introduction of ions into the sessile droplet.³⁵ In our experiments, the mechanical motion of the droplets and their influence of the flux profile are responsible for the signal changes. Additional examples of these transients are shown in Figure S4. We find that nanodroplets can perturb the diffusion layer (and therefore the measured current) either by traversing through it or by coalescing with a droplet whose boundary is very near or touching the electrode surface. After perturbation, the diffusion layer can relax which is evident by a limiting current response. The expected diffusion layer relaxation is on the order of 50 ms (electrode radius²/diffusion coefficient). From Figure 3, it takes about 50 - 100 ms to return to a limiting current after a coalescence event, though droplet rearrangement is likely also occurring after coalescence. The timescales discussed are limited by our sample rate (50 ms).

Our results highlight the importance of the environment immediately around the microelectrode. Figure S5 provides a table of schematics to illustrate the five collision events that we have now described. By using correlated microscopy, we show how the water droplet interacts with the diffusion layer, glass, and other, adsorbed water droplets to provide these characteristic responses in the current-time trace. The hydrophilicity of the glass creates an environment for droplet coalescence as the droplets collide and pack, creating large pools of water on the electrode. These pools are evident in the micrographs.

We further explore the effect of the hydrophilicity of the surrounding glass on the unexpected transients observed in amperometry by making the glass surface hydrophobic. We modified the glass of the microelectrode with dichlorodimethylsilane, a hydrophobic molecule that covalently bonds to glass. The resultant surface is methylated and much more hydrophobic than borosilicate. As shown in Figure S6A-B, the wetting angle of a pipetted 1 µL water droplet increased from about 25° to 95° after the unmodified microelectrode was silanized. Figure S6C-D shows micrographs (30 s into a collision experiment) of the unmodified glass surrounding the

microelectrode surface (Figure S6C), and micrographs where the glass was modified with the hydrophobic silane (Figure S6D). The adsorbed water droplets on silanized glass are distinct, spherical droplets whereas the adsorbed water on unmodified borosilicate is pooled in various shapes and sizes.

Representative amperograms are shown in Figure 4A (additional amperograms are shown in Figure S7), showing the difference in the electrochemical response depending on the hydrophilicity of the surrounding glass. Here, when the glass is methylated and hydrophobic, the expected staircase blocking response is observed in the amperogram. We see nearly a complete removal of the transient blocking followed by extra current events. For amperometry experiments performed using microelectrodes with unmodified glass, these transients comprise more than 30% of the observed current events. Figure 4B illustrates the two pathways for droplet adsorption and the electrochemical signal that arises. The transient blocking followed by extra current is caused by the water preferring to wet the glass insulator and is diminished by the hydrophobic modification. We suggest that when a droplet approaches the three-phase boundary (microelectrode|glass|DCE interface), it is now more likely to preferentially wet the microelectrode, manifesting in a sustained current decrease in the amperogram.

Even after many collisions, when droplets have already adsorbed to the three-phase boundary, the incoming droplet tends to coalesce, causing the adsorbed water to further wet the microelectrode and also result in a step down in current (Figure S8). We note that self-assembled monolayer modifications to the gold microelectrode with various thiols has previously been used to influence the particle dynamics at the interface.³⁶ Here we show that simple modifications to the surrounding surface can also be used to influence the adsorption of nanodroplets to a microelectrode.

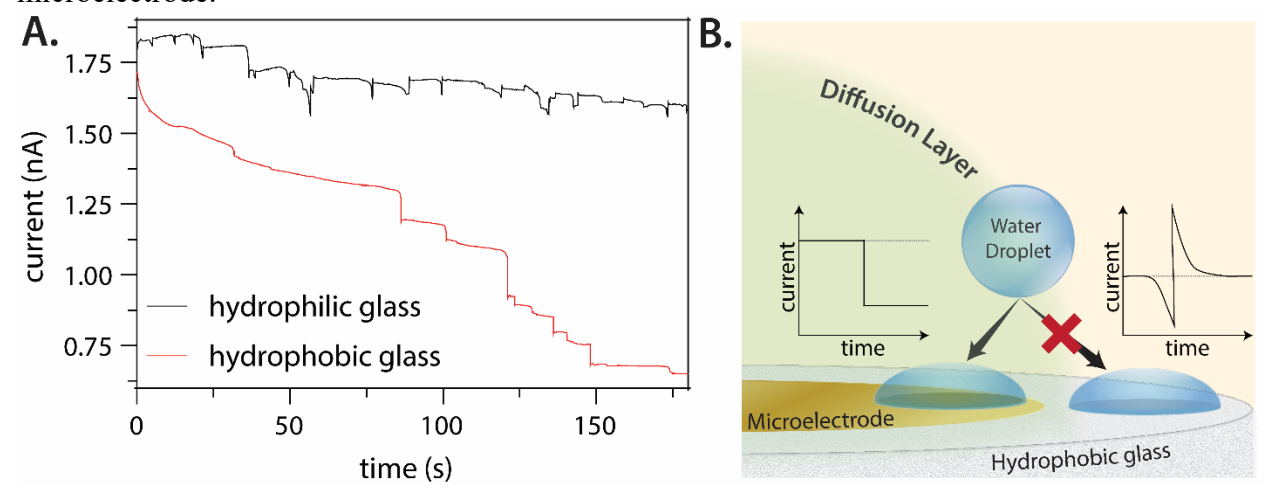


Figure 4. (A) 40 μ L of water suspended in 1 mM decmethylferrocene in 5 mM TBAP DCE. 0.3 V vs salt bridge|Ag/AgCl was applied to a gold microelectrode and salt bridge|Ag/AgCl reference (sample rate = 50 ms). The black trace shows a measurement obtained with a gold microelectrode where the glass insulation is hydrophilic and the red trace shows an amperogram obtained with a gold microelectrode where the glass insulation is hydrophobic. (B) Schematic illustrating the pathways for droplet adsorption to the microelectrode or glass at the three-phase boundary microelectrode|hydrophobic glass|DCE). The yellow represents decamethylferrocene in DCE and the green diffusion layer represents the heterogenous oxidation from decamethylferrocene to decamethylferrocenium in DCE. The scheme illustrates that droplet adsorption to the glass is eliminated by the silane treatment.

Conclusion:

In this study, we demonstrated that the collisions of water nano- and microdroplets suspended in oil do not only appear as the expected current blockade steps. We used correlated opto-electrochemical measurements to demonstrate that electrochemical transients arise from droplet-droplet coalescence events and droplets preferentially adsorbing on the glass rather than the electrode. Modifying the glass with a hydrophobic species, dimethyldichlorosilane, prevented preferential adsorption and rectified the expected current blockade response. Our results highlight the importance of 1.) the environment immediately around the microelectrode and 2.) using correlated optical microscopy to better understand collision transients.

<u>Supporting Information:</u> Cyclic voltammograms taken in the continuous phase, typical amperograms from the collision experiments, electrode-covering wetting event, more examples of droplets colliding with adsorbed water, schematics of observed collision events, micrographs of water adsorbed on unmodified and silane-treated microelectrodes.

<u>Acknowledgements:</u> Research reported in this publication was supported by the Chemical Measurement and Imaging Program in the National Science Foundation Division of Chemistry under Grant CHE-2003587.

<u>Competing Financial Interest Statement:</u> The authors declare no competing financial interests.

<u>Author Contributions:</u> KJV, CR, and JED designed experiments. KJV performed all electrochemical experiments. CR and KJV performed correlated experiments. KJV, CR, and JED wrote the manuscript. All authors agreed to the final version of this manuscript.

References:

- 1. Glasscott, M. W.; Pendergast, A. D.; Goines, S.; Bishop, A. R.; Hoang, A. T.; Renault, C.; Dick, J. E. Electrosynthesis of high-entropy metallic glass nanoparticles for designer, multi-functional electrocatalysis. *Nature Communications* **2019**, *10* (1), 2650. DOI: 10.1038/s41467-019-10303-z.
- 2. Liu, Z.; Amin, H. M. A.; Peng, Y.; Corva, M.; Pentcheva, R.; Tschulik, K. Facet-Dependent Intrinsic Activity of Single Co3O4 Nanoparticles for Oxygen Evolution Reaction. *Advanced Functional Materials* n/a (n/a), 2210945. DOI: 10.1002/adfm.202210945.
- 3. Eng, A. Y. S.; Ambrosi, A.; Sofer, Z.; Šimek, P.; Pumera, M. Electrochemistry of Transition Metal Dichalcogenides: Strong Dependence on the Metal-to-Chalcogen Composition and Exfoliation Method. *ACS Nano* **2014**, *8* (12), 12185-12198. DOI: 10.1021/nn503832j.
- 4. Pumera, M. Impact Electrochemistry: Measuring Individual Nanoparticles. *ACS Nano* **2014**, *8* (8), 7555-7558. DOI: 10.1021/nn503831r.
- 5. Jeun, Y. E.; Baek, B.; Lee, M. W.; Ahn, H. S. Surfactant-free electrochemical synthesis of metallic nanoparticles via stochastic collisions of aqueous nanodroplet reactors. *Chemical Communications* **2018**, *54* (72), 10052-10055, 10.1039/C8CC05760E. DOI: 10.1039/C8CC05760E.

- 6. Glasscott, M. W.; Dick, J. E. Electrodeposition in aqueous nanoreactors. *Current Opinion in Electrochemistry* **2021**, *25*, 100637. DOI: https://doi.org/10.1016/j.coelec.2020.09.004.
- 7. Deng, Z.; Renault, C. Unravelling the last milliseconds of an individual graphene nanoplatelet before impact with a Pt surface by bipolar electrochemistry. *Chemical Science* **2021**, *12* (37), 12494-12500, 10.1039/D1SC03646G. DOI: 10.1039/D1SC03646G.
- 8. Dick, J. E.; Renault, C.; Bard, A. J. Observation of Single-Protein and DNA Macromolecule Collisions on Ultramicroelectrodes. *Journal of the American Chemical Society* **2015**, *137* (26), 8376-8379. DOI: 10.1021/jacs.5b04545.
- 9. Zhang, J.-H.; Zhou, Y.-G. Nano-impact electrochemistry: Analysis of single bioentities. *TrAC Trends in Analytical Chemistry* **2020**, *123*, 115768. DOI: 10.1016/j.trac.2019.115768.
- 10. Vannoy, K. J.; Lee, I.; Sode, K.; Dick, J. E. Electrochemical quantification of accelerated FADGDH rates in aqueous nanodroplets. *Proc Natl Acad Sci U S A* **2021**, *118* (25). DOI: 10.1073/pnas.2025726118.
- 11. Quinn, B. M.; van't Hof, P. G.; Lemay, S. G. Time-Resolved Electrochemical Detection of Discrete Adsorption Events. *Journal of the American Chemical Society* **2004**, *126* (27), 8360-8361. DOI: 10.1021/ja0478577.
- 12. Moazzenzade, T.; Yang, X.; Walterbos, L.; Huskens, J.; Renault, C.; Lemay, S. G. Self-Induced Convection at Microelectrodes via Electroosmosis and Its Influence on Impact Electrochemistry. *Journal of the American Chemical Society* **2020**, *142* (42), 17908-17912. DOI: 10.1021/jacs.0c08450.
- 13. Thorgaard, S. N.; Jenkins, S.; Tarach, A. R. Influence of Electroosmotic Flow on Stochastic Collisions at Ultramicroelectrodes. *Analytical Chemistry* **2020**, *92* (18), 12663-12669. DOI: 10.1021/acs.analchem.0c02889.
- 14. Kim, B.-K.; Kim, J.; Bard, A. J. Electrochemistry of a Single Attoliter Emulsion Droplet in Collisions. *Journal of the American Chemical Society* **2015**, *137* (6), 2343-2349. DOI: 10.1021/ja512065n.
- 15. Cheng, W.; Compton, R. G. Oxygen Reduction Mediated by Single Nanodroplets Containing Attomoles of Vitamin B12: Electrocatalytic Nano-Impacts Method. *Angewandte Chemie International Edition* **2015**, *54* (24), 7082-7085. DOI: 10.1002/anie.201501820.
- 16. Cheng, W.; Compton, R. G. Quantifying the Electrocatalytic Turnover of Vitamin B12-Mediated Dehalogenation on Single Soft Nanoparticles. *Angewandte Chemie* **2016**, *128* (7), 2591-2595.
- 17. Miao, R.; Shao, L.; Compton, R. G. Single entity electrochemistry and the electron transfer kinetics of hydrazine oxidation. *Nano Research* **2021**, *14* (11), 4132-4139. DOI: 10.1007/s12274-021-3353-8.
- 18. Yang, H.-j.; Kwon, H.; Kim, B.-K.; Park, J. H. Electrochemical detection of single attoliter aqueous droplets in electrolyte-free organic solvent via collision events. *Electrochimica Acta* **2019**, *320*, 134620. DOI: 10.1016/j.electacta.2019.134620.

- 19. Zhang, H.; Sepunaru, L.; Sokolov, S. V.; Laborda, E.; Batchelor-McAuley, C.; Compton, R. G. Electrochemistry of single droplets of inverse (water-in-oil) emulsions. *Physical Chemistry Chemical Physics* **2017**, *19* (24), 15662-15666, DOI: 10.1039/C7CP03300A.
- 20. Dunevall, J.; Fathali, H.; Najafinobar, N.; Lovric, J.; Wigström, J.; Cans, A.-S.; Ewing, A. G. Characterizing the Catecholamine Content of Single Mammalian Vesicles by Collision—Adsorption Events at an Electrode. *Journal of the American Chemical Society* **2015**, *137* (13), 4344-4346. DOI: 10.1021/ja512972f.
- 21. Azimzadeh Sani, M.; Tschulik, K. Unveiling colloidal nanoparticle properties and interactions at a single entity level. *Current Opinion in Electrochemistry* **2022**, 101195. DOI: https: 10.1016/j.coelec.2022.101195.
- 22. Chung, H. J.; Lee, J.; Hwang, J.; Seol, K. H.; Kim, K. M.; Song, J.; Chang, J. Stochastic Particle Approach Electrochemistry (SPAE): Estimating Size, Drift Velocity, and Electric Force of Insulating Particles. *Analytical Chemistry* **2020**, *92* (18), 12226-12234. DOI: 10.1021/acs.analchem.0c01532.
- 23. Dick, J. E.; Hilterbrand, A. T.; Boika, A.; Upton, J. W.; Bard, A. J. Electrochemical detection of a single cytomegalovirus at an ultramicroelectrode and its antibody anchoring. *Proc Natl Acad Sci U S A* **2015**, *112* (17), 5303-5308. DOI: 10.1073/pnas.1504294112.
- 24. Lebègue, E.; Anderson, C. M.; Dick, J. E.; Webb, L. J.; Bard, A. J. Electrochemical Detection of Single Phospholipid Vesicle Collisions at a Pt Ultramicroelectrode. *Langmuir* **2015**, *31* (42), 11734-11739. DOI: 10.1021/acs.langmuir.5b03123.
- 25. Gao, G.; Wang, D.; Brocenschi, R.; Zhi, J.; Mirkin, M. V. Toward the Detection and Identification of Single Bacteria by Electrochemical Collision Technique. *Analytical Chemistry* **2018**, *90* (20), 12123-12130. DOI: 10.1021/acs.analchem.8b03043.
- 26. Kim, B.-K.; Boika, A.; Kim, J.; Dick, J. E.; Bard, A. J. Characterizing Emulsions by Observation of Single Droplet Collisions—Attoliter Electrochemical Reactors. *Journal of the American Chemical Society* **2014**, *136* (13), 4849-4852. DOI: 10.1021/ja500713w.
- 27. Hoang, N. T. T.; Ho, T. L. T.; Park, J. H.; Kim, B.-K. Detection and Study of Single Water/Oil Nanoemulsion Droplet by Electrochemical Collisions on an Ultramicroelectrode. *Electrochimica Acta* **2017**, *245*, 128-132. DOI: 10.1016/j.electacta.2017.05.135.
- 28. Pendergast, A. D.; Renault, C.; Dick, J. E. Correlated Optical–Electrochemical Measurements Reveal Bidirectional Current Steps for Graphene Nanoplatelet Collisions at Ultramicroelectrodes. *Analytical Chemistry* **2021**, *93* (5), 2898-2906. DOI: 10.1021/acs.analchem.0c04409.
- 29. Pendergast, A. D.; Deng, Z.; Maroun, F.; Renault, C.; Dick, J. E. Revealing Dynamic Rotation of Single Graphene Nanoplatelets on Electrified Microinterfaces. *ACS Nano* **2021**, *15* (1), 1250-1258. DOI: 10.1021/acsnano.0c08406.
- 30. ProductInformation. Aldrich, S., Ed.

- 31. Deng, Z.; Renault, C. Detection of individual insulating entities by electrochemical blocking. *Current Opinion in Electrochemistry* **2021**, *25*, 100619. DOI: 10.1016/j.coelec.2020.08.001.
- 32. Fosdick, S. E.; Anderson, M. J.; Nettleton, E. G.; Crooks, R. M. Correlated Electrochemical and Optical Tracking of Discrete Collision Events. *Journal of the American Chemical Society* **2013**, *135* (16), 5994-5997. DOI: 10.1021/ja401864k.
- 33. Ahmed, J. U.; Lutkenhaus, J. A.; Alam, M. S.; Marshall, I.; Paul, D. K.; Alvarez, J. C. Dynamics of Collisions and Adsorption in the Stochastic Electrochemistry of Emulsion Microdroplets. *Analytical Chemistry* **2021**, *93* (22), 7993-8001. DOI: 10.1021/acs.analchem.1c01027.
- 34. Park, H.; Park, J. H. In Situ Monitoring of Collision and Recollision Events of Single Attoliter Droplets via Single-Entity Electrochemistry. *J Phys Chem Lett* **2020**, *11* (23), 10250-10255. DOI: 10.1021/acs.jpclett.0c02723
- 35. Trojánek, A.; Samec, Z. Study of the emulsion droplet collisions with the polarizable water/1,2-dichloroethane interface by the open circuit potential measurements. *Electrochimica Acta* **2019**, 299, 875-885. DOI: 10.1016/j.electacta.2019.01.041.
- 36. Chen, H.-B.; Jiang, D.; Zhou, X.-L.; Qian, C.; Yang, Y.; Liu, X.-W. Tracking Interfacial Dynamics of a Single Nanoparticle Using Plasmonic Scattering Interferometry. *Analytical Chemistry* **2020**, *92* (19), 13327-13335. DOI: 10.1021/acs.analchem.0c02624.

For Table of Contents Only:

